

# Comprehensive Analysis of the Object Detection Pipeline on UAVs

Leon Amadeus Varga<sup>1</sup>, Sebastian Koch<sup>2</sup> and Andreas Zell<sup>3</sup>

**Abstract**—An object detection pipeline comprises a camera that captures the scene and an object detector that processes these images. The quality of the images directly affects the performance of the object detector. Many works nowadays focus either on improving the image quality or improving the object detection models independently, but neglect the importance of joint optimization of the two subsystems. In this paper, we first empirically analyze the influence of seven parameters (quantization, compression, resolution, color model, image distortion, gamma correction, additional channels) in remote sensing applications. For our experiments, we utilize three UAV data sets from different domains and a mixture of large and small state-of-the-art object detector models to provide an extensive evaluation of the influence of the pipeline parameters. Additionally, we realize an object detection pipeline prototype on an embedded platform for an UAV and give a best practice recommendation for building object detection pipelines based on our findings. We show that not all parameters have an equal impact on detection accuracy and data throughput, and that by using a suitable compromise between parameters we are able to improve detection accuracy for lightweight object detection models, while keeping the same data throughput.

## I. INTRODUCTION

Micro Aerial Vehicles (MAVs) and Unmanned Aerial Vehicles (UAVs) can support surveillance tasks in many applications. Example are traffic surveillance in urban environments [38], or search and rescue missions in maritime environments [32], or the much more general task of remote sensing object detection [10]. Two key components of these tasks are the camera system and the object detector. The interaction, which is normally based on image data, of these components is crucial. This work analyzes the impact of image data settings. Similar analyses are only available for the advanced driver assistance system (ADAS) scenario (see section II).

In most projects, the configuration of these components has to be conducted at an early stage. A recording of a necessary data set should be already done with the final camera system. This leads to a chicken-and-egg problem. The optimal configuration is highly application dependant, therefore we provide some critical design choices.

The emerging trend towards smart cameras, combining the



Fig. 1. Prototype system using an optimized detection pipeline.

camera and the computing unit, confirms the need for classification and detection pipelines. The lack of flexibility and the high price of these devices are still a serious drawback and prevent their use in research or prototyping. In this work, the detection pipeline is analyzed without smart cameras, but the results could also be useful for projects that include them. Besides the experiments (in a desktop and embedded environment) and the result analysis, we applied the outcomes to build a proof-of-concept system. We provide the full list of the experiments and the code<sup>4</sup>. In this work, we provide the most important findings. Our contributions are:

- We evaluated the impact of 7 parameters on three different data sets and four models.
- We provide a best practice recommendation for the parameters for the UAV object detection.
- Finally, we demonstrate the usability by building a prototype.

## II. RELATED WORK

The image processing pipeline has a large impact on the performance of object detectors. Many parameters influence this pipeline. However, there is still a lack of impact analysis for UAV-based systems. Yahyanejad *et al.* has measured the impact of lens distortion correction for thermal images acquired by a UAVs [35]. However, their results are only useful for a thermal camera system.

Other existing camera parameter evaluations are mostly based on the autonomous driving scenario [2], [7], [20], [21],

<sup>\*</sup>This work has been supported by the German Ministry for Economic Affairs and Energy, Project Avalon, FKZ: 03SX481B. Further the Training Center Machine Learning, Tübingen has been used for the evaluation (01—S17054).

<sup>1</sup>Cognitive Systems, University of Tuebingen, Germany  
leon.varga@uni-tuebingen.de

<sup>2</sup>Cognitive Systems, University of Tuebingen, Germany  
se.koch@student.uni-tuebingen.de

<sup>3</sup>Cognitive Systems, University of Tuebingen, Germany  
andreas.zell@uni-tuebingen.de

<sup>4</sup>Additional information can be found: <https://bit.ly/3KFxv7w>

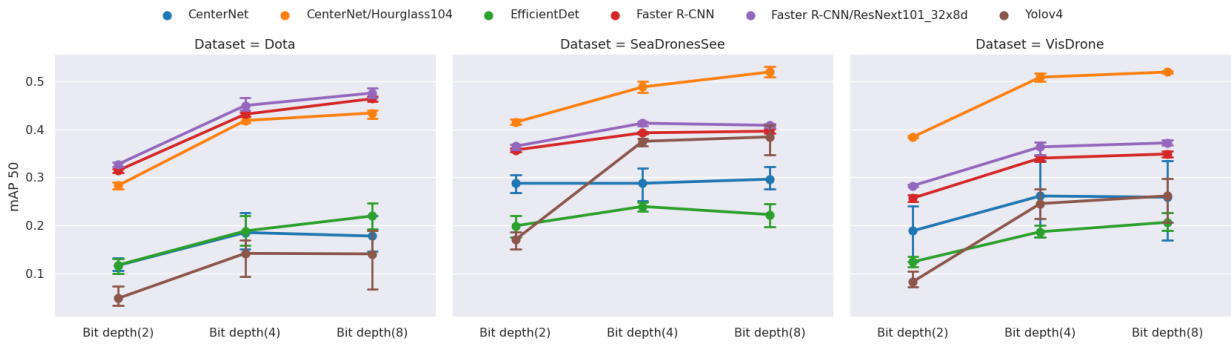


Fig. 2. Quantization: the impact of the quantization on the performance of the object detectors for all data sets. The y-axis shows the mean Average Precision (mAP).

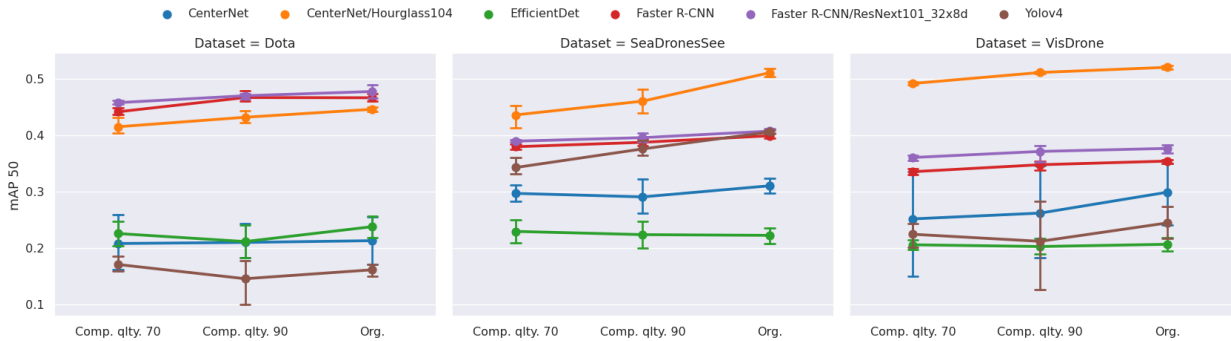


Fig. 3. Compression: the impact of the JPEG compression on the performance of the object detectors for all data sets. The y-axis shows the mean Average Precision (mAP). A higher compression quality means less compression.

[26], [27]. The findings of the autonomous driving experiments cannot be directly applied to the remote sensing use-case. For autonomous driving, the scene is often homogeneous, and the object sizes differ only slightly. Further, the distance to the objects is often only a couple of meters. For remote sensing recordings, the distance to the scene is often over 30 meters [32], resulting in tiny objects. Depending on the camera angle, the images can vary strongly. Because of these differences, the results of one scenario are not completely valid in the other, but can give a first sign.

Balsinski *et al.* proposed a render framework to evaluate camera architectures in simple autonomous driving scenarios [2]. Secci *et al.* evaluated camera failures in the autonomous driving application [27]. Besides these, the works of Liu *et al.* [20], Carlson *et al.* [7] and Saad *et al.* [26] showed the still existing gap between synthetic and real-world data. Thus, our experiments are based entirely on real-world recordings. Buckler *et al.* analyzed the image pipeline regarding performance and energy consumption [5]. In contrast to their work, we close the gap for a missing camera parameter evaluation in the remote sensing application. Further, we consider parameters, which are configurable for most off-the-shelf camera systems.

In contrast to work that accelerates inference by, e.g., quantizing the neural network [17], [6], our work focuses on the parameters of the object recognition pipeline that affect the

overall throughput time of the system, rather than on the inference time itself.

In summary, our work differs from the aforementioned works in the following aspects:

- We focus on the remote sensing use-case for UAVs.
- Instead of synthetic data, we use established real-world data sets.
- The evaluated camera parameters are configurable for most camera systems.

### III. CONSIDERED FACTORS OF INFLUENCE

Our goal is to evaluate the impact of adjustable acquisition parameters on the performance of object detectors in UAV remote sensing. We selected parameters which have a direct influence on the recordings. Three parameters, *Quantization*, *Compression* and *Resolution*, control the required memory consumption. Further, we evaluated the impact of errors of common correction methods like *Image Distortion* or invalid *Gamma Correction*. Thus, we check how important the calibration is. Further, we evaluate the impact of the selected *Color Model*. *Additional Channels* can carry useful information; we therefore check how easily they can be integrated into existing architectures and whether they help to improve the prediction capability.

There are many more relevant parameters, but we limit our evaluation to these. They have a direct influence on the

recording, but are still often easy to adjust. Our goal is to provide reliable reasons for these design choices.

#### A. Quantization

The quantization, also called bit depth for images, defines the number of different values per pixel and color. Quantization is used to describe a continuous signal with discrete values [12]. Too few quantization steps lead to a large quantization error, which results in a loss of information. Therefore, it is necessary to find a balance between the required storage space and the information it contains.

All used data sets provide images with a bit depth of 8bit per color channel. We want to evaluate, whether we can reduce the bit depth further without losing performance. This could reduce the data size. Hence, 8bit is the maximal available quantization of the data sets. We provide experiments for 8bit, 4bit and 2bit quantization.

#### B. Compression

Compression is used to reduce the required space of a recording. There are two types of compressions: lossless and lossy compressions. The image format PNG belongs to lossless compressions techniques. The compression time for PNG is very high, therefore it is often not considered for online compression. JPEG is faster, but also a lossy compression. The compression removes information. Nevertheless, JPEG is a common choice. It provides a sufficient trade-off between loss of information, file size and speed.

The compression quality of JPEG is defined as a value between 1 and 100 (default: 90). Higher values mean less compression.

We check the relation between compression and detector performance. A lower compression quality would cause smaller file sizes. This could directly lead to a higher throughput of the system. For the inferences of models, the decompressed data is used. A lower compression quality would, therefore, mainly affect the throughput from the camera to the processing unit memory. Since this is also a limiting factor for high-resolution or high-speed cameras, it is worth checking. In our experiments, we evaluate the influence of no compression and a compression quality for JPEG of 90 and 70.

#### C. Resolution

Higher resolutions reveal more details, but also result in larger recordings. Especially for the small objects of remote sensing, the details are crucial [19]. Therefore, choosing an optimal resolution is important [29].

Besides the maximal available resolution defined by the used camera, the GPU memory often limits the training size. The reason lies in the gradient calculation within the backpropagation step. There are techniques, which can reduce this problem [33], [22]. To allow a fair comparison, we limit the maximum training size to 1024 pixels for the length of the larger side. This training size is processable with all models used. The experiments should show the performance reduction for smaller image sizes. So we trained

on the training sizes of 256 pixels, 512 pixels, 756 pixels and 1024 pixels. Further, we evaluated each training size with three test sizes, which are defined by the training size  $\times$  the factors 0.5, 1 and 2.

#### D. Color Model

The color model defines the representation of the colors. One of the most common one is RGB [14]. It is an additive color model, which is based on the three colors red, green, and blue. For object detection and object classification, this representation is mostly used [25], [30]. Besides RGB, non-linear transformations of RGB are also worth considering. HLS and HSV are based on a combination of hue and saturation. Both differ only in the brightness's definition value. YCbCr takes human perception into account and encodes information more suitably for the human eye.

In some applications, HSV outperforms RGB. Cucchiara *et al.* [8] and Shuhua *et al.* [28] could confirm this performance improvement. Kim *et al.* demonstrated RGB outperforms the other color models (HSV, YCbCr, and CIE Lab) in traffic signal detection. It appears, which color model is best depends strongly on the application and the model.

The color model is also a design decision, so we evaluate the performance of the RGB, HSV, HLS, and YCbCr color models for object detection in remote sensing. We also review the performance of gray-scale images. To achieve comparable results, the backbones are not pre-trained for these experiments.

#### E. Image Distortion

During the image formation process, most lenses introduce a distortion in the digital image that does not exist in the scene [15]. Wide-angle lenses or fish-eye lenses suffer from the so-called barrel-distortion. Telephoto lenses suffer from the so-called pincushion-distortion.

Often, one of the first steps in the image processing pipeline is to correct the lens distortion using a reference pattern.

As we are working on data sets that are distortion rectified, we artificially introduce distortion via the Brown–Conrady model [4]. To evaluate the impact of an incorrect calibration, we introduce a small barrel-distortion with  $k_1 = -0.2$  and pincushion-distortion with  $k_1 = 0.2$ . A visualization of these distortions can be found in the additional material<sup>4</sup>.

#### F. Gamma Correction

Gamma Correction is a non-linear operation to encode and decode luminance to optimize the usage of bits when storing an image, by taking advantage of the non-linear manner in which humans perceive light and color [24]. Gamma Correction can also simulate a shorter or longer exposure process after the image formation process. If images are not gamma-corrected, they allocate too many bits for areas that humans cannot differentiate. Neural networks, however, differ from humans in the sense that they work with floating-point numbers which are linearly separable while humans perceive changes in brightness logarithmically. We therefore assume that Gamma Correction may have a negligible impact

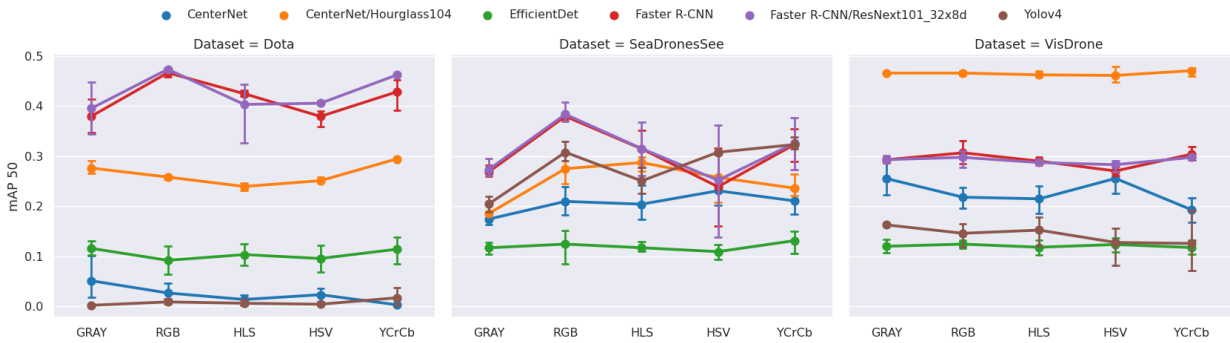


Fig. 4. Color Model: the impact of the color models on the performance of the object detectors for all data sets. The y-axis shows the mean Average Precision (mAP).

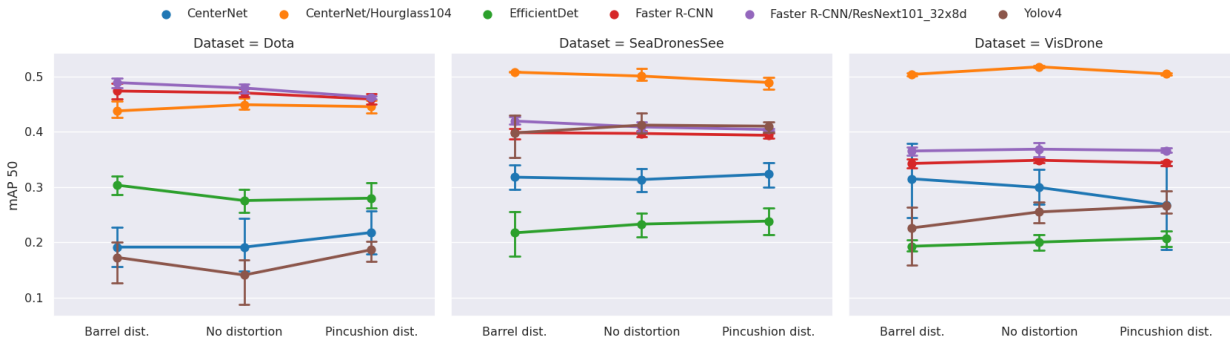


Fig. 5. Image Distortion: the impact of the image distortion on the performance of the object detectors for all data sets. The y-axis shows the mean Average Precision (mAP).

on neural network detection performance.

Many works have employed Gamma Correction, intending to improve detection performance directly or help training with Gamma Correction as an augmentation technique [34], [36].

We use three different gamma configurations (0.5, 1.0, 2.5) to investigate the effects of gamma on the object detector performance. These experiments are designed to show whether gamma is a crucial parameter. The performance of a dynamic gamma adjustment [1] will also be tested.

### G. Additional Channels

Additional Channels increase the recording size, but can also provide important information. In contrast to conventional RGB cameras, multispectral cameras record additional channels outside visible light. Very common are near infrared, red edge or thermal channels. In pedestrian and traffic monitoring, multispectral imaging can increase the detector performance, as shown by Takumi *et al.* [16], Maarten *et al.* [31], and Dayan *et al.* [13]. The focus here is not on evaluating multimodal models [23], and we consider multispectral images as a limiting case to classical color images. Therefore, experiments here are limited to the early fusion approach [37].

We used the multispectral images from the SeaDronesSee [32] data set for our experiments. These were acquired with

a MicaSense RedEdge MX and thus provide wavelengths of 475 nm (blue), 560 nm (green), 668 nm (red), 717 nm (red edge), and 842 nm (near infrared). We evaluate how the additional wavelengths affect the performance of the object detectors in detecting swimmers. The results of these experiments are not general and can only be applied to the maritime environment.

## IV. EXPERIMENTS

In this section, we describe the setup of the experiments. The setup contains the real-world data sets, the object detectors and the hardware environment. For each configuration, we trained with three different random seeds. The random seed affects the weight initialization, the order of the training samples and data augmentation techniques. The three initializations show the stability of each configuration.

### A. Datasets

We evaluated our experiments on three data sets. All data sets are part of the remote sensing scenario. Dota-2 is based on satellite recordings [10]. VisDrone [38] and SeaDronesSee [32] were recorded by Micro Air Vehicles (MAVs). The first two data sets are well established and commonly used to benchmark object detection for remote sensing. In contrast, SeaDronesSee focuses on a maritime environment, which differs from the urban environment of VisDrone and Dota-2. Therefore, it introduces new challenges and is a proper

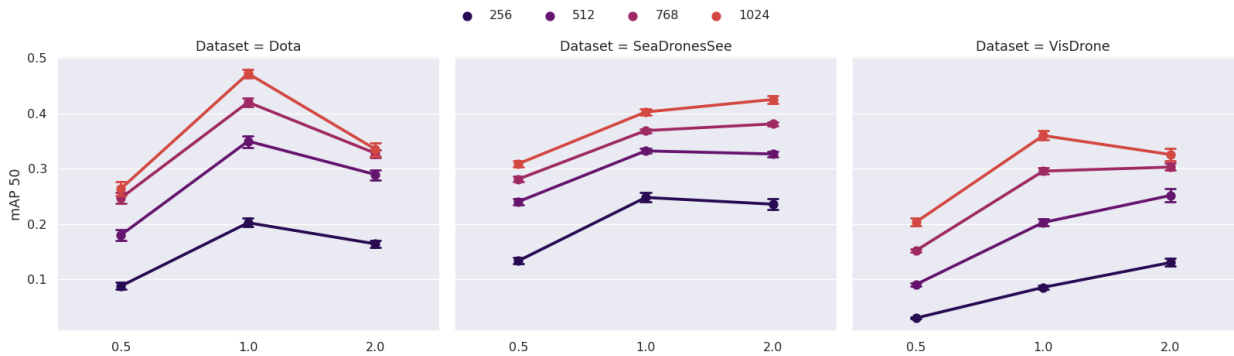


Fig. 6. Image Size: Faster R-CNN trained with different training image sizes and validated on validation image size =  $x \times$  training image size. The y-axis shows the mean Average Precision (mAP).

extension for our experiments. Further details can be found in the additional material<sup>4</sup>.

### B. Models

For our experiments, we selected four different object detectors. The two-stage detector Faster-RCNN [25] can still achieve state-of-the-art results with smaller modifications [38]. By comparison, the one-stage detectors are often faster than the two-stage detectors. Yolov4 [3] and EfficientDet [30] are one-stage detectors and focus on efficiency. Both perform well on embedded hardware. Modified versions of CenterNet [11], also a one-stage detector, could achieve satisfying results in the VisDrone challenge [38]. These four models cover a variety of approaches and can give a reliable impression of the parameter impacts.

For Faster R-CNN, EfficientDet and CenterNet, we used multiple backbones to provide an insight for different network sizes. The networks and their training procedure are described in the additional material<sup>4</sup> in further detail.

### C. Hardware setup

Most of the experiments were done in a desktop environment. To evaluate the performance in a more applicable environment, we performed experiments on an Nvidia Xavier AGX board. The small size and the low weight allow the usage for onboard processing in MAVs or other robots. The full description of the desktop and embedded environment can be found in the additional information<sup>4</sup>.

## V. RESULTS AND DISCUSSION

In this section, we present the results of the experiments. Each parameter is considered in its own subsection. The experiments of the different backbones per network were grouped, only the largest backbones of CenterNet and Faster R-CNN are listed separately. As an evaluation metric for the object detectors, we use the mean Average Precision (mAP) with an IoU threshold of 0.5 [18].

In the Dota dataset, the performance of the models differs from the performance in the other datasets. The objects in the Dota dataset are very small, unlike the other datasets. This requires different properties of the object detectors. For

a more detailed analysis of this behavior and a complete list of all experiments, we refer the reader to supplementary material<sup>4</sup>. Here we highlight the most important results in terms of parameters.

### A. Quantization

A quantization reduction leads to a loss of information in the recording. This assumption is confirmed by the empirical results in Fig. 2. This phenomenon is consistent for all data sets and all models. However, deterioration varies. Worth mentioning is the marginal difference ( $\sim 3\%$ ) in performance between 4bit and 8bit recordings. Hence, it is possible to have half the amount of data and achieve nearly the same result. The loss in performance for a 2bit quantization is much higher ( $\sim 41\%$ ).

### B. Compression

Fig. 3 shows the relation between compression quality and object detector performance. Lower compression quality, i.e. higher compression, leads to worse performance. With some exceptions, this is true for all models. Overall, the performance degeneration of the tested compression qualities is small. For a compression quality of 90, the performance is decreased by  $\sim 2.7\%$ . A compression quality of 70 leads to an mAP loss of  $\sim 5.3\%$ . Compared to the performance loss, the size reduction is significant.

We observe that a compression quality of 90 reduces the required space by  $\sim 25\%$  for a random subset of the VisDrone validation set. A compression quality of 70 can almost halve the required space.

However, the memory reduction depends highly on the image content. For SeaDronesSee and Dota the memory reduction is much higher. For compression quality of 70 and 90, it is about  $\sim 93\%$  and,  $\sim 86\%$  respectively.

By reducing the required image space, it is possible to increase the pipeline throughput. In return, a compression and decompression is necessary. In the final experiments (see VI), the utility of this approach becomes clear.

### C. Color Model

We can conclude two important outcomes of the experiment for color models. First, we have to distinguish between

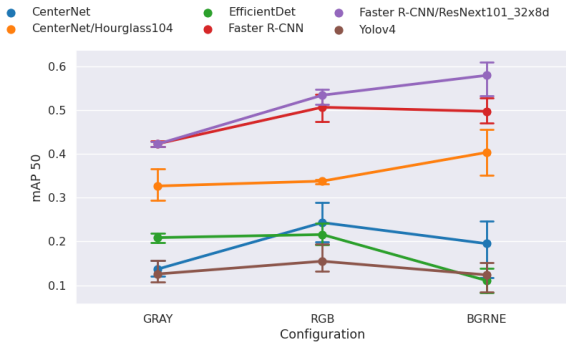


Fig. 7. Multispectral: the improvement of the performance of the object detectors with multispectral data (SeaDronesSee-multispectral). The y-axis shows the mean Average Precision (mAP). ‘BGRNE’ indicates the performance on the multispectral recordings. ‘RGB’ and ‘GRAY’ represent the performance on color and gray-scale images.

two situations, which are visible in Fig. 4. In the first situation, the object detectors seem to not take advantage of the color information. Therefore, we assume the color is in this case not beneficial. This applies to the VisDrone data set and for the Dota data set. Both data sets provide objects and backgrounds with a high color variance. For example, a car in the VisDrone data set can have any color. Thus, the texture is much more important. That means the object detector can already achieve excellent results with the gray-scale recordings. For the Dota data set, the color information could only be used by the largest models (Faster R-CNN/ResNext101\_32x8d and CenterNet/Hourglass104). The other models weren’t able to incorporate the color and relied only on the texture.

In our SeaDronesSee experiments, we observe that the gray-scale experiments are outperformed by the color experiments. The explanation can be found in the application. It covers a maritime environment. As a result, the background is always a mixture of blue and green. So, the color information is reliable in distinguishing between background and foreground. For SeaDronesSee, all models use the color, which is evident in the drop in performance for the gray-scale experiments. If the color is important, RGB seems to produce the overall best results; followed by YCrCb. However, since most data augmentation pipelines have been optimized for RGB, it is recommended to start with RGB.

As a conclusion, it is important to know whether color information is relevant in the application. Most times, gray-scale images are sufficient, which leads to a third of the image size and may even allow simpler cameras.

#### D. Image Distortion

The results of the distortion experiments are visible in Fig. 5. Runs that were trained and tested on images with barrel-distortion perform the best or on par with no distortion across all models for Dota and SeaDronesSee, except for EfficientDet and the CenterNet with smaller backbones. Sometimes even pincushion-distortion shows better, but still very similar, results than no distortion. We assume this is

TABLE I

GAMMA CORRECTION: OVERALL IMPACT ON THE PERFORMANCE.

	Gamma(0.5)	Original	Gamma(2.5)	Dynamic
Relative mAP50 $\uparrow$	98.9 %	<b>100 %</b>	98.3 %	99.2 %

because these data sets comprise small objects, where the image distortion does not affect the shape of the objects much. Sometimes even, the distortion might be helpful, as with barrel-distortion and pincushion-distortion areas of the image get magnified, which could lead to better detection performance if objects lie in these areas.

To conclude, we can reason with these experiments that a small distortion does not have a negative impact on detection performance in remote sensing object detection.

#### E. Gamma Correction

The overall results of the experiments (visible in Tab. I, normalized with respect to the original performance) show that Gamma Correction seems not to have a large impact on detector performance. We notice, however, that dynamic Gamma Correction seems to have either no effect or a negative effect. We reason it is not important, for a neural network, whether an image is slightly under or overexposed.

#### F. Resolution

For these experiments, we only visualize the experiments of Faster R-CNN. The three selected plots (visible in Fig. 6) are good representatives for the other models, because they describe the general behavior well. The full list of experiments can be found in the additional material<sup>4</sup>.

First, higher training resolutions always improve the performance of the models. Aside from that, the deterioration of performance for a decreased validation image size is consistent.

For the Dota data set, we can observe a performance drop for a higher scale factor. The trained models seem very sensitive to object sizes and cannot take advantage of higher resolutions.

For the SeaDronesSee data set, performance improves with higher validation image sizes for most models. So it is possible to improve the performance of a trained model by simply using higher inference resolutions. However, the improvement is marginal and should be supported by scaling data augmentation.

The results for the SeaDronesSee data set also apply to the VisDrone data set. Only for the training image size of 1024 pixels, this rule does not hold. The reason for this is the small number of high-resolution images in the VisDrone validation set. In summary, training and validation size seems to be crucial, and it is not a good idea to cut corners at this point.

#### G. Additional Channels

These experiments are based on multispectral data of the SeaDronesSee data set. The set of about 500 multispectral images is not very large, so the results can only give an impression. The usefulness of the additional channels depends

TABLE II  
APPLICATION OF THE OPTIMIZED PARAMETER CONFIGURATION IN A DESKTOP AND AN EMBEDDED ENVIRONMENT.

Data set	Dota mAP 50 ↑	VisDrone mAP 50 ↑	SeaDronesSee mAP 50 ↑	avg. Throughput FPS ↑ (Desktop)	avg. Throughput FPS ↑ (Embedded)	Number of Parameters
EfficientDet	23.83	20.71	22.29	25	14	
Reduced data (our) *	22.07 (-7 %)	19.53 (-5 %)	22.20 (-1 %)	<b>28 (+12 %)</b>	<b>16 (+14 %)</b>	4.5M - 17.7 M
Reduced data + higher resolution (our) **	<b>30.85 (+ 29%)</b>	<b>25.52 (+23 %)</b>	<b>27.35 (+23 %)</b>	25	14	
YoloV4	16.19	24.49	40.62	20	4	63.9M
Reduced data (our) *	13.84 (-14 %)	23.61 (-3 %)	36.58 (-9 %)	<b>21 (+5 %)</b>	<b>5 (+20 %)</b>	
CenterNet	21.35	29.94	31.08	40	-	14.4M - 49.7 M
Reduced data (our) *	21.22 (-1 %)	27.87 (-6 %)	31.05 (-1 %)	<b>46 (+15 %)</b>	-	
CenterNet/Hourglass104	44.63	52.07	51.12	6	-	200M
Reduced data (our) *	41.15 (-7 %)	48.59 (-6 %)	47.89 (-6 %)	6	-	
Faster R-CNN	46.67	35.45	39.94	17	-	41.4M - 60.3M
Reduced data (our) *	43.92 (-5 %)	33.05 (-6 %)	39.26 (-1 %)	<b>18 (+6 %)</b>	-	
Faster R-CNN/ResNext101_32x8d	47.78	37.70	40.76	9	-	104M
Reduced data (our) *	44.06 (-7 %)	35.87 (-4 %)	40.59 (-1 %)	9	-	

strongly on the application. For the maritime environment, the additional information is very useful, especially the near-infrared channel. This part of the spectrum is absorbed by water [9], resulting in a foreground mask.

The results in Fig. 7 fit to the findings for the color models (see section V-C). For the maritime environment, the color is important, indicated by the gap for gray-scale recordings. The multispectral recordings (labeled as ‘BGRNE’) can only improve the performance of the larger models. For the smaller models, it even leads to a decrease in performance. To support the multispectral recordings as input, we had to increase the input-channels of the first layer to five. The rest of the backbone is still pre-trained.

In summary, additional channels can be helpful depending on the use case. It is important to keep in mind that larger backbones can make better use of the additional information. Furthermore, it is a trade-off between a fully pre-trained backbone and additional channels.

## VI. APPLICATION

Based on the previous investigations, we determined the optimal parameter configuration for our application. The goal was to find a suitable compromise between the performance of the object detector and the required space for a recording. The size of the recording correlates directly with the throughput of the camera and the object detector, including the inference time. A smaller recording size therefore means more frames per second during detection.

We considered the following points:

- 1) A quantization reduction from 8bit to 4bit seems easy to apply.
- 2) A JPEG compression with a compression quality of 90 reduces the performance only slightly.
- 3) For the urban surveillance use-case, color is not important. Thus, for the VisDrone data set, we used gray-scale images. For the other data sets, the color is important.
- 4) Keep the highest possible resolution, because this is a crucial parameter for small objects.

- 5) The images of the data sets have already been rectified and gamma corrected. As has been shown, a minor error is not critical.

In Tab. II, the application of these findings is visible. The first setup (marked \*), which uses the points 1), 2) and 3), increases the throughput (including the inference, the pre- and post-processing) of the smaller models significantly. For the larger models, inference accounts for most of the throughput, so there is no significant speed increase here.

By combining the previous three items and item 4) (marked \*\*), the performance of the detector can be improved while maintaining the base throughput. In these experiments, the usage of CroW [33] allowed training with higher resolution. Finally, we use the findings to deploy a UAV based prototype (displayed in Fig. 1) with nearly real-time and high-resolution processing. The system was carried by a DJI Matrice 100 drone. An Nvidia Xavier AGX board (Jetpack version 4.6), mounted on the drone, performed the calculations. We used TensorRT (8.0.1) to optimize the model efficiency with a floating point precision of 16. The ‘‘MAXN’’ power mode of the Nvidia Xavier was used to enable the maximum GPU clock rate of 1377 MHz. A GenICam compatible camera by the manufacture Allied Vision was used (Allied Vision 1800 U-1236).

## VII. CONCLUSION

This paper presents an extensive study of parameters that should be considered when designing a full object detection pipeline in an UAV use-case. Our experiments show that not all parameters have an equal impact on detection performance, and a trade-off can be made between detection accuracy and data throughput.

By using the above recommendations, 1) to 5), it is possible to maximize the efficiency of the object detection pipeline in a remote sensing application.

More parameters might be considered in future work. Also, a deeper analysis of the usability of multispectral imaging could provide useful insights.

## REFERENCES

- [1] M. Abdullah-Al-Wadud, Md. Hasanul Kabir, M. Ali Akber Dewan, and Oksam Chae. A dynamic histogram equalization for image contrast enhancement. *IEEE Transactions on Consumer Electronics*, 53(2):593–600, 2007.
- [2] Henryk Blasinski, Joyce E. Farrell, Trisha Lian, Zhenyi Liu, and Brian A. Wandell. Optimizing image acquisition systems for autonomous driving. *electronic imaging*, 2018:161–1–161–7, 2018.
- [3] Alexey Bochkovskiy, Chien-Yao Wang, and Hong-Yuan Mark Liao. Yolov4: Optimal speed and accuracy of object detection. *CoRR*, abs/2004.10934, 2020.
- [4] Duane C Brown. Decentering distortion of lenses. *Photogrammetric Engineering and Remote Sensing*, 1966.
- [5] Mark Buckler, Suren Jayasuriya, and Adrian Sampson. Reconfiguring the imaging pipeline for computer vision. In *IEEE International Conference on Computer Vision, ICCV 2017, Venice, Italy, October 22-29, 2017*, pages 975–984. IEEE Computer Society, 2017.
- [6] Yaohui Cai, Zhewei Yao, Zhen Dong, Amir Gholami, Michael W. Mahoney, and Kurt Keutzer. Zeroq: A novel zero shot quantization framework. In *2020 IEEE/CVF Conference on Computer Vision and Pattern Recognition, CVPR 2020, Seattle, WA, USA, June 13-19, 2020*, pages 13166–13175. Computer Vision Foundation / IEEE, 2020.
- [7] Alexandra Carlson, Katherine A. Skinner, Ram Vasudevan, and Matthew Johnson-Roberson. Modeling camera effects to improve visual learning from synthetic data. In Laura Leal-Taixé and Stefan Roth, editors, *Computer Vision - ECCV 2018 Workshops - Munich, Germany, September 8-14, 2018, Proceedings, Part I*, volume 11129 of *Lecture Notes in Computer Science*, pages 505–520. Springer, 2018.
- [8] R. Cucchiara, C. Grana, M. Piccardi, A. Prati, and S. Sirotti. Improving shadow suppression in moving object detection with hsv color information. In *ITSC 2001. 2001 IEEE Intelligent Transportation Systems. Proceedings (Cat. No.01TH8585)*, pages 334–339, 2001.
- [9] Joseph A. Curcio and Charles C. Petty. The near infrared absorption spectrum of liquid water. *J. Opt. Soc. Am.*, 41(5):302–304, May 1951.
- [10] Jian Ding, Nan Xue, Gui-Song Xia, Xiang Bai, Wen Yang, Michael Ying Yang, Serge J. Belongie, Jiebo Luo, Mihai Datcu, Marcello Pelillo, and Liangpei Zhang. Object detection in aerial images: A large-scale benchmark and challenges. *CoRR*, abs/2102.12219, 2021.
- [11] Kaiwen Duan, Song Bai, Lingxi Xie, Honggang Qi, Qingming Huang, and Qi Tian. Centernet: Keypoint triplets for object detection. In *2019 IEEE/CVF International Conference on Computer Vision, ICCV 2019, Seoul, Korea (South), October 27 - November 2, 2019*, pages 6568–6577. IEEE, 2019.
- [12] A. Gersho. Quantization. *IEEE Communications Society Magazine*, 15(5):16–16, 1977.
- [13] Dayan Guan, Yanpeng Cao, Jiangxin Yang, Yanlong Cao, and Michael Ying Yang. Fusion of multispectral data through illumination-aware deep neural networks for pedestrian detection. *Inf. Fusion*, 50:148–157, 2019.
- [14] R.W.G. Hunt. *The Reproduction of Colour*. The Wiley-IS&T Series in Imaging Science and Technology. Wiley, 2005.
- [15] Photography — Digital cameras — Geometric distortion (GD) measurements. Standard, International Organization for Standardization, Geneva, CH, July 2015.
- [16] Takumi Karasawa, Kohei Watanabe, Qishen Ha, Antonio Tejero-de-Pablos, Yoshitaka Ushiku, and Tatsuya Harada. Multispectral object detection for autonomous vehicles. In Wanmin Wu, Jianchao Yang, Qi Tian, and Roger Zimmermann, editors, *Proceedings of the on Thematic Workshops of ACM Multimedia 2017, Mountain View, CA, USA, October 23 - 27, 2017*, pages 35–43. ACM, 2017.
- [17] Rundong Li, Yan Wang, Feng Liang, Hongwei Qin, Junjie Yan, and Rui Fan. Fully quantized network for object detection. In *IEEE Conference on Computer Vision and Pattern Recognition, CVPR 2019, Long Beach, CA, USA, June 16-20, 2019*, pages 2810–2819. Computer Vision Foundation / IEEE, 2019.
- [18] Tsung-Yi Lin, Michael Maire, Serge J. Belongie, James Hays, Pietro Perona, Deva Ramanan, Piotr Dollár, and C. Lawrence Zitnick. Microsoft COCO: common objects in context. In David J. Fleet, Tomás Pajdla, Bernt Schiele, and Tinne Tuytelaars, editors, *Computer Vision - ECCV 2014 - 13th European Conference, Zurich, Switzerland, September 6-12, 2014, Proceedings, Part V*, volume 8693 of *Lecture Notes in Computer Science*, pages 740–755. Springer, 2014.
- [19] Kang Liu and Gellért Mátyus. Fast multiclass vehicle detection on aerial images. *IEEE Geosci. Remote. Sens. Lett.*, 12(9):1938–1942, 2015.
- [20] Zhenyi Liu, Trisha Lian, Joyce E. Farrell, and Brian A. Wandell. Soft prototyping camera designs for car detection based on a convolutional neural network. In *2019 IEEE/CVF International Conference on Computer Vision Workshops, ICCV Workshops 2019, Seoul, Korea (South), October 27-28, 2019*, pages 2383–2392. IEEE, 2019.
- [21] Zhenyi Liu, Trisha Lian, Joyce E. Farrell, and Brian A. Wandell. Neural network generalization: The impact of camera parameters. *IEEE Access*, 8:10443–10454, 2020.
- [22] Martin Messmer, Benjamin Kiefer, and Andreas Zell. Gaining scale invariance in UAV bird’s eye view object detection by adaptive resizing. *CoRR*, abs/2101.12694, 2021.
- [23] Tanguy Ophoff, Kristof Van Beeck, and Toon Goedemé. Exploring rgb+depth fusion for real-time object detection. *Sensors*, 19(4):866, 2019.
- [24] Charles Poynton. *Digital video and HD: Algorithms and Interfaces*. Elsevier, 2012.
- [25] Shaoqing Ren, Kaiming He, Ross B. Girshick, and Jian Sun. Faster R-CNN: towards real-time object detection with region proposal networks. *IEEE Trans. Pattern Anal. Mach. Intell.*, 39(6):1137–1149, 2017.
- [26] Kmeid Saad and Stefan-Alexander Schneider. Camera vignetting model and its effects on deep neural networks for object detection. In *2019 IEEE International Conference on Connected Vehicles and Expo, ICCVE 2019, Graz, Austria, November 4-8, 2019*, pages 1–5. IEEE, 2019.
- [27] Francesco Secci and Andrea Ceccarelli. On failures of RGB cameras and their effects in autonomous driving applications. In Marco Vieira, Henrique Madeira, Nuno Antunes, and Zheng Zheng, editors, *31st IEEE International Symposium on Software Reliability Engineering, ISSRE 2020, Coimbra, Portugal, October 12-15, 2020*, pages 13–24. IEEE, 2020.
- [28] Li Shuhua and Guo Gaizhi. The application of improved hsv color space model in image processing. In *2010 2nd International Conference on Future Computer and Communication*, volume 2, pages V2–10–V2–13, 2010.
- [29] Mingxing Tan and Quoc V. Le. Efficientnet: Rethinking model scaling for convolutional neural networks. In Kamalika Chaudhuri and Ruslan Salakhutdinov, editors, *Proceedings of the 36th International Conference on Machine Learning, ICML 2019, 9-15 June 2019, Long Beach, California, USA*, volume 97 of *Proceedings of Machine Learning Research*, pages 6105–6114. PMLR, 2019.
- [30] Mingxing Tan, Ruoming Pang, and Quoc V. Le. Efficientdet: Scalable and efficient object detection. In *2020 IEEE/CVF Conference on Computer Vision and Pattern Recognition, CVPR 2020, Seattle, WA, USA, June 13-19, 2020*, pages 10778–10787. Computer Vision Foundation / IEEE, 2020.
- [31] Maarten Vandersteegen, Kristof Van Beeck, and Toon Goedemé. Real-time multispectral pedestrian detection with a single-pass deep neural network. In Aurélio Campilho, Fakhri Karray, and Bart M. ter Haar Romeny, editors, *Image Analysis and Recognition - 15th International Conference, ICIAR 2018, Póvoa de Varzim, Portugal, June 27-29, 2018, Proceedings*, volume 10882 of *Lecture Notes in Computer Science*, pages 419–426. Springer, 2018.
- [32] Leon Amadeus Varga, Benjamin Kiefer, Martin Messmer, and Andreas Zell. Seadronesee: A maritime benchmark for detecting humans in open water. In *Proceedings of the IEEE/CVF Winter Conference on Applications of Computer Vision*, pages 2260–2270, 2022.
- [33] Leon Amadeus Varga and Andreas Zell. Tackling the background bias in sparse object detection via cropped windows. In *Proceedings of the IEEE/CVF International Conference on Computer Vision (ICCV) Workshops*, pages 2768–2777, October 2021.
- [34] Chuan-Wei Wang, Chin-An Cheng, Ching-Ju Cheng, Hou-Ning Hu, Hung-Kuo Chu, and Min Sun. Augpod: Augmentation-oriented probabilistic object detection. In *CVPR Workshop on the Robotic Vision Probabilistic Object Detection Challenge*, 2019.
- [35] Saeed Yahyanejad, Jakub Misiorny, and Bernhard Rinner. Lens distortion correction for thermal cameras to improve aerial imaging with small-scale uavs. In *2011 IEEE International Symposium on Robotic and Sensors Environments, ROSE 2012, Montréal, Canada, September 17-18, 2011*, pages 231–236. IEEE, 2011.
- [36] Lili Zhang, Yi Zhang, Zhen Zhang, Jie Shen, and Huibin Wang. Real-time water surface object detection based on improved faster r-cnn. *Sensors*, 19(16):3523, 2019.
- [37] Yifei Zhang, Désiré Sidibé, Olivier Morel, and Fabrice Mériaudeau. Deep multimodal fusion for semantic image segmentation: A survey. *Image Vis. Comput.*, 105:104042, 2021.
- [38] Pengfei Zhu, Longyin Wen, Dawei Du, Xiao Bian, Qinghua Hu, and Haibin Ling. Vision meets drones: Past, present and future. *CoRR*, abs/2001.06303, 2020.